The strength of the 3′-*gauche* effect dictates the structure of 3′-*O*-anthraniloyladenosine and its 5′-phosphate, two analogues of the 3′-end of aminoacyl-tRNA

Parag Acharya,[a] Barbara Nawrot,[b] Mathias Sprinzl,[c] Christophe Thibaudeau[a] and Jyoti Chattopadhyaya *[a]

[a] *Department of Bioorganic Chemistry, Box 581, Biomedical Centre, University of Uppsala, S-751 23 Uppsala, Sweden. E-mail: jyoti@bioorgchem.uu.se. Fax: +4618554495*
[b] *Laboratory of Bioorganic Chemistry, Polish Academy of Sciences Centre of Molecular and Macromolecular Studies 90-363 Lodz, Sienkiewicza 112, Poland*
[c] *Laboratorium für Biochemie, Universität Bayreuth, 95440 Bayreuth, Germany*

Received (in Cambridge) 30th November 1998, Accepted 14th April 1999

Anthranilic acid charged yeast tRNA^{Phe} or *E. coli* tRNA^{Val} are able to form a stable complex with EF-Tu*GTP, hence the 2′- and 3′-*O*-anthraniloyladenosines and their 5′-phosphate counterparts have been conceived to be the smallest units that are capable of mimicking aminoacyl-tRNA. Since the 3′-*O*-anthraniloyladenosine also binds more efficiently to the EF-Tu*GTP complex compared to its 2′-isomer, we have herein delineated the stereoelectronic features that dictate the conformation of 3′-*O*-anthraniloyladenosine and its 5′-phosphate *vis-a-vis* their 2′-counterparts and we have also addressed how their structures and thermodynamic stabilizations are different from adenosine and 5′-AMP. It has been found that the electron-withdrawing anthraniloyl group exerts *gauche* effects of variable strengths depending upon whether it is at the 2′- or at 3′-position because of either the presence or absence of O2′–N9 *gauche* effect, [GE(O2′–C2′–C1′–N9)], thereby steering the pseudorotation of the constituent sugar moiety either to the North (N)-type (C3′-*endo*) or South (S)-type (C2′-*endo*) conformation. The 3′-*O*-anthraniloyladenosine 5′-phosphate has a relatively more stabilized S-type conformation $\Delta G^\circ = -4.6$ kJ mol^{-1}) than 3′-*O*-anthraniloyladenosine itself ($\Delta G^\circ = -3.9$ kJ mol^{-1}), whereas the ΔG° for 2′-*O*-anthraniloyladenosine and its 5′-monophosphate are respectively -0.9 and -1.8 kJ mol^{-1}, suggesting that the 3′-*gauche* effect of the 3′-*O*-anthraniloyl group is stronger than that of 2′-*O*-anthraniloyl in the drive of the sugar conformation. Since the EF-Tu can specifically recognize the aminoacylated-tRNA from the non-charged tRNA, we have assessed the free-energy (ΔG°) for this recognition switch to be the least ≈ -2.9 kJ mol^{-1} by comparison of ΔG° of the N⇌S pseudorotational equilibrium for 3′-*O*-anthraniloyladenosine 5′-phosphate and 5′-AMP. The 3′-*O*-anthraniloyladenosine and its 5′-phosphate are much more flexible than the isomeric 2′-counterparts as is evident from the temperature-dependent coupling constants analysis. The relative rate of the transacylation reaction of 2′(3′)-*O*-anthraniloyladenosine and its 5′-phosphate is cooperatively dictated by the two-state N⇌S pseudorotational equilibrium of the sugar, which in turn is controlled by a balance of the stereoelectronic 3′- and 2′-*gauche* effects as well as by the pseudoaxial preference of the 3′-*O*- or 2′-*O*-anthraniloyl group. The reason for the larger stabilization of the 2′-*endo* conformer for 3′-*O*-anthraniloyladenosine and its 5′-phosphate lies in the fact that the C3′–O3′ bond takes up an optimal *gauche* orientation with respect to the C4′–O4′ bond dictating the pseudoaxial orientation of the 3′-anthraniloyl residue, which can be achieved only in the S-type sugar conformation with adenin-9-yl and the 2′-OH groups in the pseudoequatorial geometry, compared to the preferred C3′-*endo* sugar with a pseudoaxial aglycone and 2′-OH found in the 3′-terminal adenosine moiety in the helical 3′-CCA end of uncharged tRNA.

Introduction

During the process of *in vivo* protein synthesis an amino acid attached to the 3′-terminal adenosine of transfer RNA (tRNA) serves as an acceptor for a peptidyl residue. In this process the aminoacylated-tRNA (aa-tRNA) which is correctly charged by a cognate aminoacyl tRNA synthetase has to specifically interact with several enzymes, protein factors such as elongation factor Tu, and the ribosome. Differences of several orders of magnitude exist in the equilibrium dissociation constants between non-aminoacylated tRNA and aminoacyl-tRNA and these macromolecules constitute the molecular basis of recognition of aminoacyladenosine on the 3′-end of aminoacyl-tRNA.[1] Despite this large difference in the equilibrium dissociation constants between non-aminoacylated tRNA and aminoacyl-tRNA in the interaction with elongation factor Tu, no large structural change was noted in tRNA upon aminoacylation.[2] It has been suggested however[3] that the destacking of the 3′-terminal adenosine upon aminoacylation is the structural element determining the recognition of aminoacyl-tRNA by the elongation factor Tu (EF-Tu)*GTP complex. At standard physiological conditions the migration of the aminoacyl residue between the 2′- and 3′-ribose positions (transacylation) in aa-tRNA takes place.[4] This means that EF-Tu must be able to distinguish between the two isomeric substrates, namely 2′- and 3′-aminoacyl-tRNA. The 3′aminoacyl-tRNA is found to bind to EF-Tu both in the solid[5] and solution[4b] state.

It has been shown that the 3′-*O*-anthraniloyladenosine, compared to its 2′-isomer, binds more efficiently to the EF-Tu*GTP complex from the eubacterium *Thermus thermophilus*.[6] Since anthranilic acid charged yeast tRNA^{Phe}[7] or *E. coli* tRNA^{Val}[8] are able to form a stable complex with EF-Tu*GTP, the 2′- and 3′-*O*-anthraniloyladenosines (Scheme 1, **1a** and **2a**) and their 5′-phosphate (Scheme 1, **1b** and **2b**) counterparts have been

Table 1 Thermodynamics (kJ mol^{-1})[a] of the pseudorotational equilibrium of the isomeric 2′- and 3′-*O*-anthraniloyladenosine and their 5′-phosphates

Compound	ΔH°[b]	$-T\Delta S^{\circ}$[b] (298 K)	ΔG°[c] 275 K	298 K	338 K	$\Delta\Delta G^{\circ}$[d,e] (298 K)
Adenosine	−4.4 (0.2)	2.6 (0.1)		−1.8 (0.2)		
5′-AMP	−3.5 (0.6)	1.8 (0.6)	1.8 (0.1)	−1.7 (0.1)	−1.4 (0.2)	
2′-ant-Ado (**1a**)	−1.3 (0.5)	−0.5 (0.5)	−1.7 (0.2)	−1.8 (0.2)	−1.7 (0.2)	0.0[d]
3′-ant-Ado (**2a**)	−5.6 (0.7)	1.7 (0.7)	−4.0 (0.2)	−3.9 (0.2)	−3.7 (0.2)	−2.1[d]
2′-ant-AMP (**1b**)	−0.3 (0.5)	−0.7 (0.5)	−0.9 (0.2)	−0.9 (0.2)	−1.0 (0.2)	+0.8[e]
3′-ant-AMP (**2b**)	−8.5 (0.8)	3.9 (0.8)	−5.0 (0.3)	−4.6 (0.3)	−3.9 (0.2)	−2.9[e]

[a] The signs of the thermodynamic parameters are chosen in such a way that the positive and negative values indicate the drive of the N⇌S equilibrium towards N-type and S-type conformations, respectively (see ref. 9). [b] ΔH° and ΔS° are average values (their standard deviations are shown in brackets) (see ref. 9 and 13). [c] ΔG° at $T = 275$ K, 298 K and 338 K have been calculated from the relation: $\Delta G^{T} = -RT \ln (x_S/x_N)$ where x_S and x_N are mole fractions of S- and N-type conformations. These values were comparable to the ΔG° calculated using the relation: $\Delta G^{T} = \Delta H^{\circ} - T\Delta S^{\circ}$. [d] $\Delta\Delta G^{\circ}$ has been calculated according to the relation: $\Delta\Delta G^{\circ} = \Delta G^{\circ}$ (298 K) of 2′- or 3′-anthraniloyl-Ado − ΔG° (298 K) of adenosine. [e] $\Delta\Delta G^{\circ}$ has been calculated according to the relation: $\Delta\Delta G^{\circ} = \Delta G^{\circ}$ (298 K) of 2′- or 3′-anthraniloyl-AMP − ΔG° (298 K) of 5′-AMP.

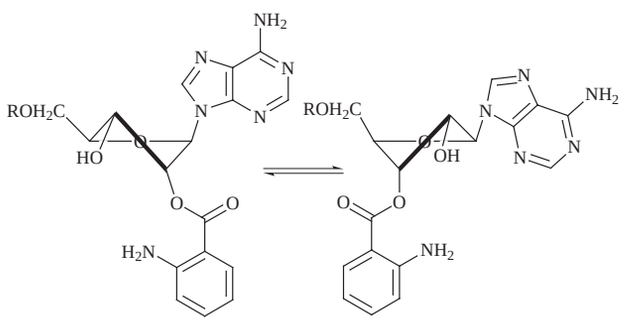

Scheme 1

conceived to be the smallest units that are capable of mimicking aa-tRNA.[6,8] Since 3′-*O*-anthraniloyladenosine binds more strongly to EF-Tu than the corresponding 2′-isomer, it has been suggested that the structure of the 3′-isomer could be a good starting point to design specific inhibitors[6] of the aa-tRNA*-EF-Tu interaction, and thus the whole bacterial protein biosynthesis. It is this latter question that has persuaded us to examine whether there are any intrinsic differences between the sugar pseudorotational behaviour of 2′-*O*-anthraniloyl- and 3′-*O*-anthraniloyladenosines (2′-ant-Ado and 3′-ant-Ado respectively) and their 5′-phosphate counterparts. Related to this, we have also debated whether the thermodynamics of the sugar pseudorotational characteristics of 2′-*O*-anthraniloyl and 3′-*O*-anthraniloyladenosines and their 5′-phosphate counterparts are indeed related to their intrinsic ability to transacylate.

In this work, we have examined the relative thermodynamics of the pseudorotation of 2′- and 3′-*O*-anthraniloyladenosines and their 5′-phosphate counterparts as well as the underlying stereoelectronic forces that thermodynamically dictate their conformational preferences in comparison with adenosine and adenosine 5′-phosphate (5′-AMP), thereby attempting to understand the energetic basis of discrimination of uncharged tRNA *vis-a-vis* aminoacylated-tRNA by the EF-Tu*GTP complex.

Results and discussion

(A) Interplay of stereoelectronic forces in the drive of the sugar conformations in nucleos(t)ides

Our earlier NMR studies[9] have uniquely shown that the two-state North (N)-type (C3′-*endo*) or South (S)-type (C2′-*endo*) pseudorotational equilibrium[10,11] of the sugar moiety in nucleos(t)ides is energetically controlled by the interplay of stereoelectronic *gauche*[9a,g,i,j,12] [$\sigma_{C-H} \rightarrow \sigma^*_{C-O/N}$ orbital mixing] and anomeric[9] [$n(O4') \rightarrow \sigma^*_{C1'-N}$ orbital mixing] effects as well as the steric effects of various substituents. It is however the electronic character, the configuration of the sugar substituents as well as their environments, in general, that dictate the relative strengths of these stereoelectronic effects.[9]

(B) Difference between the energetics of 3′-*O*-anthraniloyladenosine and its 5′-phosphate and their 2′-counterparts

The population of S-type conformations in 3′-*O*-anthraniloyladenosine and in its 5′-phosphate decreases with increasing temperature (see Experimental section (B) for details of pseudorotational analyses[9,13] of sugar conformations and Experimental section (C) for van't Hoff plots). There is a net decrease of 6 and 10% x_S for 3′-*O*-anthraniloyladenosine and its 5′-phosphate, respectively, on going from 275 to 338 K.[9,13] However, in the case of the 2′-isomer of both adenosine as well as its 5′-phosphate, the sugar conformation is locked in a 60 : 40 ratio of S- and N-type sugars over the whole temperature range. A van't Hoff plot of ln (x_S/x_N) *versus* the inverse of temperature for the 3′-*O*-anthraniloyladenosine as well as its 5′-phosphate gave straight lines.[9a,s] The slope and the intercept gave ΔH°, $-\Delta S^{\circ}$ as well as ΔG° (Table 1). Since there was very little temperature dependency of ln (x_S/x_N) in 2′-*O*-anthraniloyladenosine and its 5′-phosphate, the van't Hoff plot was much less accurate and the error in the determination of the thermodynamic quantities was high (Table 1).

(C) Comparison of the strengths of the 2′- and 3′-*gauche* effects in 2′- and 3′-*O*-anthraniloyladenosines and their 5′-phosphates

In 2′- and 3′-*O*-anthraniloyladenosines and their 5′-phosphate counterparts, the anomeric and inherent steric effects of adenin-9-yl are present in all four derivatives, and hence can be disregarded in this relative assessment of the stereoelectronic forces that drive their respective sugar pseudorotations. There is however an interplay of three different *gauche* effects (GE) in both 2′- and 3′-isomers: GE[O2′–C2′–C1′–N9], GE[O2′–C2′–C1′–O4′] and GE[O3′–C3′–C4′–O4′], which play a key role in the modulation of the thermodynamics of the two-state N⇌S equilibrium. In this dynamic N⇌S conformational equilibrium, the influence of GE[O2′–C2′–C3′–O3′] can also be assumed to be mutually cancelled, since it is present in both 2′- and 3′-isomers.

We have earlier shown[9] that GE[O2′–C2′–C1′–N9] and GE[O3′–C3′–C4′–O4′] drive the sugar conformation towards the S-type, whereas GE[O2′–C2′–C1′–O4′] drives the sugar to the N-type. Hence the electronic nature governing the strength of the relative electronegatives of the substituent attached to

the 2′- or 3′-position will either enhance or weaken the strength of the 2′- or 3′-GE,[9a,g,i,j] and this will be the decisive factor in the outcome of the *gauche* effect promoted drive of the overall N⇌S equilibrium.

Due to its stronger electron-withdrawing nature, the anthraniloyl group exerts *gauche* effects of variable strengths depending upon whether it is located at the 2′- or 3′-position because this will influence the presence or absence of GE[O2′–C2′–C1′–N9]. The strength of the 2′- or 3′-*gauche* effects of the anthraniloyl group in **1a**,**b** and **2a**,**b**, and thereby the effect of the 2′- or 3′-aminoacylation in general, can be assessed in comparison with the hydroxy group by comparing the effect of the former with the latter in adenosine or 5′-AMP. Owing to the stereoelectronic nature of a pure *gauche* interaction,[12] it should be independent of the overall entropy of the system, which is difficult to delineate in practice. As accurate estimate of the relative magnitude of the pure stereoelectronic 3′- and 2′-*gauche* effects in **1a**,**b** and **2a**,**b** in comparison with adenosine or 5′-AMP can be simply derived[9a,i,j] by subtracting the respective $\Delta H°$ values to give $\Delta\Delta H°$ (eqns. (1a) and (2a)), whereas the overall effect of substitution of the anthraniloyl group in **1a**,**b** and **2a**,**b** compared with 2′/3′-OH in adenosine or 5′-AMP can only be assessed by the relative change of stabilization of S- over N-type pseudorotamers by subtracting their respective $\Delta G°$ values to give $\Delta\Delta G°$ (eqns. (1b) and (2b)). Thus the relative strengths of the 2′- or 3′-*gauche* effects of the anthraniloyl group ($\Delta\Delta G°$) in **1a**,**b** and **2a**,**b** can be quantified.

$$\Delta\Delta H° = [\Delta H° \text{ (298 K) of 2′- or 3′-ant-Ado}] - [\Delta H° \text{ (298 K) of adenosine}] \quad (1a)$$

$$\Delta\Delta G° \text{ (at 298 K)} = [\Delta G° \text{ (298 K) of 2′- or 3′-ant-Ado}] - [\Delta G° \text{ (298 K) of adenosine}] \quad (1b)$$

$$\Delta\Delta H° = [\Delta H° \text{ (298 K) of 2′- or 3′-ant-AMP}] - [\Delta H° \text{ (298 K) of 5′-AMP}] \quad (2a)$$

$$\Delta\Delta G° \text{ (at 298 K)} = [\Delta G° \text{ (298 K) of 2′- or 3′-ant-AMP}] - [\Delta G° \text{ (298 K) of 5′-AMP}] \quad (2b)$$

Thus, $\Delta\Delta H°$ ($\Delta\Delta G°$) values for 2′-*O*-anthraniloyladenosine 5′-phosphate and 2′-*O*-anthraniloyladenosine are respectively 3.2 (+0.8) and 3.1 (0.0) kJ mol^{-1}, whereas $\Delta\Delta G°$ for their 3′-counterparts are respectively −5.0 (−2.9) and −1.2 (−2.1) kJ mol^{-1}, showing that the 3′-*O*-anthraniloyl group exerts a stronger *gauche* effect than the 2′-*O*-anthaniloyl group. The reason for the weaker *gauche* effect of the 2′-*O*-anthraniloyl group is that its actual strength is reduced by the competing GE[O2′–C2′–C1′–N9] and GE[O2′–C2′–C1′–O4′], which are absent for the 3′-*O*-anthraniloyl group.

In the case of 2′-*O*-anthraniloyladenosine 5′-phosphate (2′-ant-AMP), a relatively stronger GE[O2′–C2′–C1′–N9] driving the sugar to the S-type conformation is counteracted by the GE[O2′–C2′–C1′–O4′], which drives the sugar to the N-type conformation. Their magnitudes are relatively similar as is evident from the 60:40 x_S/x_N sugar population, which translates into $\Delta G° = -0.9$ kJ mol^{-1} (at 298 K, including the contribution of the anomeric effect) for the drive of the N⇌S equilibrium to the S-type. Similarly in the case of 2′-*O*-anthraniloyladenosine (2′-ant-Ado), the relatively stronger GE[O2′–C2′–C1′–N9] driving the sugar to the S-type conformation is counteracted by the GE[O2′–C2′–C1′–O4′], which drives the sugar to the N-type conformation. Their magnitudes are relatively comparable in 2′-ant-Ado, and we find a $\Delta G°$ (298 K) = −1.8 kJ mol^{-1} (Table 1) favouring slightly an S-type conformation. Remarkably, the $\Delta G°$ of the N⇌S equilibrium of both 2′-ant-AMP and 2′-ant-Ado are temperature independent over the 275–338 K range, thereby showing poor flexibility in its structural make-up, which is also evidenced from counteracting values for $\Delta H°$ and $-T\Delta S°$ (Table 1).

However, in the case of 3′-*O*-anthraniloyladenosine 5′-phosphate (3′-ant-AMP) both GE[O3′–C3′–C4′–O4′] and GE[O2′–C2′–C1′–N9] drive the sugar conformation towards the S-type, whereas the GE[O2′–C2′–C1′–O4′] drives the sugar conformation to the N-type. Here it is noteworthy that it is the GE[O3′–C3′–C4′–O4′] which is the most dominating driving force to the preferred S-type conformation (90% S, 10% N in the N⇌S equilibrium) because of the stronger electronegativity of the 3′-*O*-anthaniloyl group, and as a result, we observe a relatively large stabilization of the S-type conformer as evident from a $\Delta G°$ (298 K) value of −4.6 kJ mol^{-1}. The drive of the sugar conformation in 3′-*O*-anthraniloyladenosine (3′-ant-Ado) is also governed by the 3′-*gauche* effect arising from the 3′-*O*-anthraniloyl group, causing a net preference for the S-type sugar ($\Delta G° = -3.9$ kJ mol^{-1}, Table 1).

The important characteristic observed here for 3′-ant-AMP or Ado derivatives *vis-a-vis* 2′-*O*-anthraniloyl counterparts is that the $\Delta G°$ is temperature-dependent: The $\Delta G°$ for 3′-ant-AMP varies from −5.0 kJ mol^{-1} at 275 K to −3.9 kJ mol^{-1} at 338 K, whereas for 3′-ant-Ado, $\Delta G°$ varies from −4.0 kJ mol^{-1} to −3.7 kJ mol^{-1} in the same temperature range, thereby showing an intrinsic structural flexibility of the 3′-isomer. It has not escaped our attention that this inherently flexible character of 3′-*O*-anthraniloyladenosine and its 5′-phosphate is perhaps a useful degree of freedom that can possibly be used by EF-Tu to steer and tune its conformation to a free-energy minimum for facilitating its recognition, interaction and binding to EF-Tu.

The second important biological consequence of the energetic preferences of 3′-*O*-anthraniloyladenosine and its 5′-phosphate compared to adenosine and 5′-AMP (compare $\Delta\Delta G°$ in Table 1) is that, upon aminoacylation, the bias of the two-state 3′-*endo* (N)⇌2′-*endo* (S) pseudorotational equilibrium shifts to the C2′-*endo* from the preferred C3′-*endo* state as found in the 3′-terminal adenosine moiety in the helical 3′-CCA end of tRNA in the free compared to the aminoacylated state. This shift of the N⇌S equilibrium to the S form is the crucial structural change of aminoacyl-tRNA compared to free tRNA. Each tRNA specific for a particular amino acid needs a cognate synthetase for its recognition, whereas once tRNA is aminoacylated, all tRNA molecules are transported by the same protein (EF-Tu) to the ribosome. Thus, the free-energy of the structural changes of the 3′-terminal adenosine moiety which occur upon aminoacylation of tRNA must serve as a recognition element for EF-Tu. The $\Delta G°$ for this switch (at 298 K) has been assessed to be ≈ −2.9 kJ mol^{-1}, obtained by subtracting the $\Delta G°$ at 298 K of the N⇌S equilibrium of 3′-*O*-anthraniloyladenosine 5′-phosphate from that of 5′-AMP.

(D) The temperature-dependency of the molar ratio of the 2′- and 3′-anthraniloyl isomers

It has been observed that the molar ratio of 2′-*O*-anthraniloyladenosine (or its 5′-phosphate) gradually increases over that of the corresponding 3′-isomer as the temperature increases from 275 K to 338 K (see Experimental section (D)). The plot of the logarithm of the ratio of 3′- over 2′-isomer as a function of the inverse of the temperature gives a straight line (see Experimental section (E)), thereby giving the thermodynamics of the isomerization process: $\Delta H° = -1.6$ kJ mol^{-1}, $-T\Delta S°$ at 298 K = 0.4 kJ mol^{-1}, and $\Delta G° = -1.2$ kJ mol^{-1} for 2′- and 3′-ant-AMP, and $\Delta H° = -1.0$ kJ mol^{-1}, $-T\Delta S°$ at 298 K = −0.7 kJ mol^{-1}, and $\Delta G° = -1.7$ kJ mol^{-1} for 2′- and 3′-ant-Ado.

(E) The ratio of mole fractions of 2′- over 3′-isomers of the anthraniloyl group and relative populations of S- and N-conformers are correlated

We then examined whether the relative rate of 2′/3′-isomerization of the anthraniloyl group is in some way related to the change of the population of the sugar conformation. Hence, we plotted the logarithm of the ratio of mole fractions of 2′/3′-

isomers of both 3′-ant-Ado and 3′-ant-AMP *versus* the logarithm of the ratio of the population of S- and N-type sugar pseudorotamers, which gave straight lines (see Experimental section (F)). These correlation plots show that as well as the increase of the population of the N-type conformer with increasing temperature, the ratio of the 2′-isomer increases (see Experimental section (F)). Similarly, as the temperature decreases, the population of the S-type conformer increases with an increase of the 3′-isomer population, because the bulky and polar 2′-anthraniloyl group takes up a pseudoaxial position in the N-type conformation whereas the 3′-anthraniloyl group becomes pseudoaxial in the S-type conformation (Scheme 1). *Thus, it is shown for the first time that the preference of a sugar conformation and the preponderance of a specific aminoacylated isomer are mutually interdependent.* It therefore follows that the 2′/3′-aminoacyl isomer equilibrium can be shifted more to the 2′-isomer by shifting the pseudorotational equilibrium to the N-type conformation by retuning the anomeric effect of the adenin-9-yl moiety in the aa-tRNA by protonation or metallation or complexation with a electrophilic ligand under given physiological conditions. This may in turn act as a switch for promoting the dissociation of enzymes and protein factors that recognize and bind to the 3′-aminoacyl isomer and the associated C2′-*endo* conformation.

Conclusions

(1) It is evident from the relative temperature dependency of the N⇌S population and from the relative preference for the S-type conformation in the 3′- and 2′-isomers of anthraniloyl-AMP or adenosine derivatives that the 3′-isomers have a relatively more stabilized S-type conformation ($\Delta G^\circ = -4.6$ kJ mol^{-1} and $\Delta G^\circ = -3.9$ kJ mol^{-1} for 3′-isomers of AMP and adenosine respectively), driving the 3′-*O*-anthraniloyl group into the pseudoaxial orientation because of the intrinsic energy-minimizing *gauche* orientation of C3′–O3′ and C4′–O4′ bonds. The 3′-aminoacyl isomers are also endowed with a larger stabilization of the 2′-*endo* conformer, and also are more inherently flexible, which allows them to play key roles in more effective enzymatic recognition by EF-Tu compared to the 2′-isomer.

(2) It has been found that the relative migration of the anthraniloyl group from the 3′- to the 2′-position is nearly the same for both the anthraniloyladenosines and their 5′-phosphate derivatives. However, the percentage change of the S-type conformation (Table 1) over the temperature range 275–338 K and ΔG° are higher for 3′-ant-AMP (-4.6 kJ mol^{-1}) than 3′-ant-Ado (-3.9 kJ mol^{-1}). This suggests that the structural modification of 3′-ant-AMP will most probably produce a better inhibitor of the aa-tRNA*EF-Tu interaction which is necessary for bacterial protein biosynthesis since the magnitude of the stabilization of the C2′-*endo* conformation most probably serves as a recognition element by elongation factor Tu.

(3) Upon aminoacylation, the bias of the two-state 3′-*endo* (N)⇌2′-*endo* (S) pseudorotational equilibrium shifts to the C2′-*endo* state in the 3′-terminal adenosine moiety in the helical 3′-CCA end of tRNA. This shift of the N⇌S equilibrium to the S form is the crucial structural change that takes place in the aminoacyl-tRNA compared to the uncharged tRNA. Each tRNA specific for a particular amino acid needs a cognate synthetase for its recognition, whereas once tRNA is aminoacylated, all tRNA molecules are transported by the same protein (EF-Tu) to ribosome. Thus, the free-energy of the structural changes of the 3′-terminal adenosine moiety which occur upon aminoacylation of tRNA must serve as a recognition element for EF-Tu. The energy penalty for this switch (ΔG° at 298 K) has been assessed to be ≈ -2.9 kJ mol^{-1} by comparison of ΔG° of the N⇌S pseudorotational equilibrium of 3′-*O*-anthraniloyladenosine 5′-phosphate and 5′-AMP.

(4) In summary, the culmination of the optimal antiperiplanar interaction between the σ orbital of the C3′–H bond and the σ* orbital of the C4′–O4′ (σ→σ* orbital mixing), resulting in an optimal *gauche* orientation of C3′–O3′ with respect to C4′–O4′, dictates the pseudoaxial orientation of the 3′-anthraniloyl residue in the S-type sugar conformation, thereby placing both the adenin-9-yl moiety and the free 2′-OH group in the pseudoequatorial positions. This simple conformational switch, orchestrated by the dynamic change of the 2′⇌3′ transacylation equilibrium, has at least three important biological consequences: (i) the aminoacylation influences the N⇌S equilibrium of the 3′-terminal adenosine, (ii) the S-type conformation of the 3′-end of aminoacyl-tRNA fits to the binding pocket of EF-Tu,[7] (iii) ligands with a predominant N-type sugar conformation, such as puromycin, cannot serve as analogs of aminoacyl-tRNA for interaction with EF-Tu.[8]

Experimental

(A) Temperature-dependent ^{1}H NMR spectra at 600 MHz

^{1}H NMR spectra were recorded for both compounds [2′(3′)-*O*-anthraniloyladenosine and 2′(3′)-*O*-anthraniloyladenosine 5′-phosphate] at 5 mM concentration at 600 MHz (Bruker DRX 600) in 0.5 ml of the following buffer solutions: 100 mM NaCl, 10 mM NaH_2PO_4, 10 mM Na_2HPO_4, 20 mM $MgCl_2$, 10 μM EDTA, pD 7.2 in 99.9% D_2O with 0.05 ml of CD_3OD as co-solvent ($\delta_{CH_3CN} = 2.00$ ppm as internal reference) between 275 K and 338 K at 5 K intervals. The pD value corresponds to the reading on a pH meter equipped with a calomel electrode calibrated with two standard buffers (pH 4 and 7) and is not corrected for the deuterium isotope effect. All spectra have been recorded using 64 K data points and 100 scans. The accurate $^3J_{HH}$ (±0.1 Hz) values (Table 2) were obtained through simulation using the DAISY program package (supplied by Bruker spectrospin, Germany) and have been used for the pseudorotational analyses [*vide infra*, section (B)].

(B) Conformational preferences of sugar moieties in 2′- and 3′-isomers of anthraniloyladenosine and its 5′-phosphate derivatives by pseudorotational analyses with PSEUROT program

The experimentally measured vicinal $^3J_{HH}$ ($^3J_{1'2'}$, $^3J_{2'3'}$, $^3J_{3'4'}$) values have been used (Table 2) as input for the PSEUROT (version 5.4) program[13] to calculate the temperature-dependent bias of the two-state N⇌S equilibrium of the sugar moieties in the 2′- and 3′-isomers of anthraniloyladenosine and its 5′-phosphate derivatives. The PSEUROT program[13] calculates the iterative best fit between the experimentally measured $^3J_{HH}$ and the five pseudorotational parameters needed to describe the two-state equilibrium[9–11] [*i.e.* the phase angles of the N (P_N) and S (P_S) pseudorotamers, their respective puckering amplitudes Ψ_m(N) and Ψ_m(S), as well as the mole fractions of one of them].

The PSEUROT program is based on the pseudorotation concept[14] and on the new generalised Karplus equation,[15a,b] which links $^3J_{HH}$ coupling constants to the corresponding proton–proton torsion angles on the basis of the "λ" substituent parameters scale.[15c,d] The following λ values have been used for the substituents attached to the H–C–C–H fragments: λ (C1′) = λ (C2′) = λ (C3′) = λ (C4′) = 0.62, λ (C5′) = 0.68, λ (O4′) = 1.27, λ (OH) = 1.26, λ (glycosyl-N) = 0.58, λ [OC(=O)R] = 1.15.[15c,d] The proton–proton torsion angles in the pentofuranose moiety can be translated into the corresponding endocyclic angles (v_i, i = 0–4) by the PSEUROT program using a relationship of the type $\Phi_{HH} = B + Av_i$. A and B parameters for all compounds are as follows: $A = 1.03$ and $B = 121.4$ for $\Phi_{1'2'}$, $A = 1.06$ and $B = 2.40$ for $\Phi_{2'3'}$, $A = 1.09$ and $B = -124.0$ for $\Phi_{3'4'}$. The PSEUROT analyses have been performed in two ways: (i) Ψ_m(N) and Ψ_m(S) were first assumed to be identical and constrained to the same value in a certain range (*vide infra*) during the PSEUROT calculation, and (ii) when either the N or the S pseudorotamers is significantly preferred over the other (*i.e.* by

Table 2 $^3J_{HH}$ couplings (in Hz) for all compounds over the temperature range 275–338 K

Compound	Coupling	275 K	278 K	283 K	288 K	293 K	298 K	303 K	308 K	313 K	318 K	323 K	328 K	333 K	338 K
2′-ant-ADO (**1a**)	$^3J_{1'2'}$	6.1	6.1	6.1	6.1	6.1	[a]	6.1	6.1	6.0	6.0	6.0	6.0	6.0	5.9
	$^3J_{2'3'}$	5.5	5.5	5.5	5.6	5.6	[a]	5.6	5.6	5.6	5.6	5.6	5.6	5.7	5.7
	$^3J_{3'4'}$	3.8	3.8	3.8	3.8	3.8	[a]	3.8	3.8	3.9	3.9	3.9	3.9	3.9	4.0
3′-ant-ADO (**2a**)	$^3J_{1'2'}$	7.2	7.2	7.2	7.1	7.1	7.1	7.1	7.0	7.0	6.9	6.9	6.9	6.8	6.8
	$^3J_{2'3'}$	5.4	5.5	5.5	5.5	5.5	5.5	5.5	5.5	5.5	5.5	5.6	5.6	5.6	5.6
	$^3J_{3'4'}$	2.3	2.4	2.4	2.4	2.5	2.5	2.6	2.6	2.7	2.7	2.8	2.8	2.9	2.9
2′-ant-AMP (**1b**)	$^3J_{1'2'}$	5.4	5.4	5.4	5.4	[a]	5.4	5.5	5.4	5.4	5.4	5.4	5.5	5.4	5.5
	$^3J_{2'3'}$	5.4	5.4	5.4	5.4	[a]	5.5	5.5	5.5	5.6	5.6	5.6	5.6	5.6	5.6
	$^3J_{3'4'}$	4.3	4.3	4.3	4.3	[a]	4.3	4.3	4.4	4.4	4.4	4.4	4.4	4.5	4.5
3′-ant-AMP (**2b**)	$^3J_{1'2'}$	7.6	7.5	7.5	7.5	7.5	7.4	7.4	7.3	7.3	7.3	7.2	7.1	7.1	7.0
	$^3J_{2'3'}$	5.2	5.2	5.2	5.2	5.3	5.3	5.3	5.3	5.3	5.3	5.4	5.4	5.4	5.4
	$^3J_{3'4'}$	1.7	1.8	1.9	1.9	1.9	2.0	2.1	2.1	2.2	2.2	2.3	2.5	2.5	2.6

[a] H2′ resonance at this temperature was under the residual HOD signal, and these coupling constants could therefore not be determined.

≥70%), P and Ψ_m of the minor conformer have been frozen to different sets of values (*vide infra*), while the geometry of the major conformer was optimized freely during the PSEUROT fitting process.

The ensemble of PSEUROT analyses performed for each compound has been designed in order to examine the hyperspace of geometries that are accessible to the N-type and S-type pseudorotamers and in such way that the deviations between the experimental and back-calculated $^3J_{HH}$ (they are reflected in the values of ΔJ_{max}, *vide infra*) as well as the rms of the analyses remain minimal (*vide infra*). We have also investigated the influence of the error (±0.1 Hz) of the experimentally measured $^3J_{HH}$ by performing various sets of PSEUROT analyses with randomization of $^3J_{HH}$ coupling values by allowing them to vary ±0.1 Hz from experimental values over the entire temperature range for all compounds. For each compound, the different sets of temperature-dependent mole fractions of the N-type or the S-type pseudorotamers were calculated during various PSEUROT optimization, which were used to make the van't Hoff plots (typically 10000 plots). The different slopes and intercepts of these van't Hoff plots were subsequently averaged to get average contributions to the N⇌S equilibrium as well as their associated standard deviations.

2′-ant-Ado. The population of S-type conformers (%S) at different temperatures are as follows (error is shown in parentheses): 68 (1.7) at 275 K, 68 (1.7) at 288 K, 68 (1.7) at 298 K, 68 (1.7) at 308 K, 66 (1.7) at 318 K, 66 (1.7) at 328 K, 65 (1.7) at 338 K. Ψ_m(N) and Ψ_m(S) have been first constrained to the same value from 30° to 45° in 1° steps. P_N and P_S, optimized during these PSEUROT analyses, are $-39° < P_N < 40°$ and $125° < P_S < 154°$.

3′-ant-Ado. The population of S-type conformers (%S) at different temperatures is as follows (error is shown in parentheses): 85 (1.3) at 275 K, 84 (1.3) at 288 K, 83 (1.3) at 298 K, 82 (1.3) at 308 K, 81 (1.3) at 318 K, 80 (1.3) at 328 K, 79 (1.3) at 338 K. Ψ_m(N) and Ψ_m(S) have been first constrained to the same value from 30° to 45° in 1° steps. P_N and P_S, optimized during these PSEUROT analyses are $-20° < P_N < 40°$ and $152° < P_S < 164°$. We have also subsequently constrained P_N to $-15° < P_N < 30°$ in 15° steps with Ψ_m(N) fixed at 34°, 36° and 38° which resulted in $152° < P_S < 163°$ with $35° < \Psi_m(S) < 38°$ ($\Delta J_{max} < 0.3$ Hz and rms < 0.2 Hz). The resulted mole fractions of the N-type and S-type conformers were used to make the van't Hoff plots.

2′-ant-AMP. The population of S-type conformers (%S) at different temperatures is as follows (error is shown in parentheses): 59 (1.5) at 275 K, 59 (1.5) at 288 K, 59 (1.5) at 298 K, 57 (1.5) at 308 K, 59 (1.5) at 318 K, 60 (1.5) at 328 K, 59 (1.5) at 338 K, Ψ_m(N) and Ψ_m(S) have been first constrained to the same value from 30° to 45° in 1° steps. P_N and P_S, optimized during these PSEUROT analyses, are $-18° < P_N < 39°$ and $163° < P_S < 131°$.

3′-ant-AMP. The population of S-type conformers (%S) at different temperatures is as follows (error is shown in parentheses): 90 (1.2) at 275 K, 88 (1.2) at 288 K, 87 (1.2) at 298 K, 85 (1.2) at 308 K, 85 (1.2) at 318 K, 81 (1.2) at 328 K, 80 (1.2) at 338 K. Ψ_m(N) and Ψ_m(S) have been first constrained to the same value from 30° to 45° in 1° steps. P_N and P_S are optimized during these PSEUROT analyses. We have also subsequently constrained P_N to $-15° < P_N < 30°$ in 15° steps with Ψ_m(N) fixed at 35°, 37° and 40° which resulted in $145° < P_S < 158°$ with $33° < \Psi_m(S) < 38°$ ($\Delta J_{max} < 0.3$ Hz and rms < 0.2 Hz). The resulting mole fractions of N-type and S-type conformers were used to draw the same number of van't Hoff plots.

(C) Van't Hoff plots of mole fractions of sugar conformations *vs.* 1/*T* for 1a and 1b

The plot of the logarithm of ratio of mole fractions of S-type conformation (x_S) and N-type conformation (x_N) [$\ln(x_S)/(x_N)$] as a function of the inverse of the temperature (1000/T) over the temperature range of 275–338 K for 3′-*O*-anthraniloyladenosine (**1a**) and 3′-*O*-anthraniloyladenosine-5′-monophosphate (**1b**) give straight lines with slope = 0.68 ($\sigma = 0.01$), intercept = −0.70 ($\sigma = 0.05$) and Pearson's correlation coefficient (R) = 0.99 for the former, and slope = 1.02 ($\sigma = 0.03$), intercept = −1.57 ($\sigma = 0.12$) and Pearson's correlation coefficient (R) = 0.98 for the latter.

(D) The temperature-dependency of the molar ratio of 2′- and 3′-anthraniloyl isomers

The molar ratio of 2′- to 3′-isomers of the anthraniloyladenosine and its 5′-phosphate derivatives at various temperatures have been achieved by integrating the H1′ of the 3′-isomer while integration of H1′ proton resonance of the 2′-isomer has been referenced as 1.0. They are as follows: 2′-(3′)-ant-AMP (**2b**)/(**1b**) 1.71 at 275 K, 1.65 at 288 K, 1.61 at 298 K, 1.56 at 308 K, 1.58 at 318 K, 1.52 at 328 K, 1.51 at 338 K. 2′-(3′)-ant-Ado (**2a**)/(**1a**) 1.94 at 275 K, 1.98 at 288 K, 1.94 at 298 K, 1.95 at 308 K, 1.91 at 318 K, 1.85 at 328 K, 1.81 at 338 K.

(E) Van't Hoff plots of mole fractions of 2′/3′-*O*-anthraniloyl isomers *vs.* 1/*T* for 1a and 1b

The plot of the logarithm of the ratio of mole fractions of the 3′-isomer (3′) and the 2′-isomer (2′) [*i.e.* ln(3′)/(2′)] as a function of the inverse of the temperature (1000/T) over the temperature range of 275–338 K for 3′-*O*-anthraniloyladenosine (**1a**) and for 3′-*O*-anthraniloyladenosine 5′-monophosphate (**1b**) give straight lines with a slope = 0.12 ($\sigma = 0.01$), intercept = 0.27 ($\sigma = 0.04$) and Pearson's correlation coefficient (R) = 0.88 for the former, and with slope = 0.19 ($\sigma = 0.01$),

intercept = −0.16 (σ = 0.02) and Pearson's correlation coefficient (R) = 0.97 for the latter.

(F) The correlation plot of sugar conformation with the ratio of 2′/3′-isomers

The plot of the logarithm of the ratio of the mole fractions of the 3′-isomers (3′) and the 2′-isomer (2′) [ln(3′)/(2′)] as a function of the logarithm of the ratio of mole fractions of the S-type conformation (x_S) and N-type conformation (x_N) [ln(x_S)/(x_N)] over the temperature range of 278–333 K for 3′-*O*-anthraniloyladenosine (**1a**) and 3′-*O*-anthraniloyladenosine 5′-monophosphate (**1b**) give straight lines with slope = 0.19 (σ = 0.01), intercept = −0.16 (σ = 0.02) and Pearson's correlation coefficient (R) = 0.82 for the former, and slope = 0.18 (σ = 0.01), intercept = 0.15 (σ = 0.02) and Pearson's correlation coefficient (R) = 0.96 for the latter.

Acknowledgements

We thank the Swedish Board for Technical Development, Swedish Natural Science Research (NFR) Council, Swedish Board for Technical Development (NUTEK), the Deutsche Forschungsgemeinschaft (Sp 243/5-3) and Fonds der Chemischen Industrie for generous financial support. Thanks are due to the Wallenbergstiftelsen, Forskningsrådsnämnden and University of Uppsala for funds for the purchase of 500 MHz and 600 MHz Bruker DRX NMR spectrometers.

References

1 F. Janiak, V. A. Dell, J. K. Abrahamson, B. S. Watson, D. L. Miller and A. E. Johnson, *Biochemistry*, 1990, **29**, 4268.
2 R. O. Potts, N. C. Ford, Jr. and M. J. Fournier, *Biochemistry*, 1981, **20**, 1653.
3 B. Nawrot, W. Milius, A. Ejchart, S. Limmer and M. Sprinzl, *Nucleic Acids Res.*, 1997, **25**, 948.
4 (*a*) M. Taiji, S. Yokoyama and T. Miyazawa, *Nucleic Acids Res.*, 1982, **11**, 161; (*b*) M. Taiji, S. Yokoyama and T. Miyazawa, *Biochemistry*, 1985, **98**, 1447.
5 P. Nissen, M. Kjeldgaard, S. Thirup, G. Polekhina, L. Reshetnikova, B. F. C. Clark and J. Nyborg, *Science*, 1995, **270**, 1464.
6 S. Limmer, M. Vogtherr, B. Nawrot, R. Hillenbrand and M. Spinzl, *Angew. Chem., Int. Ed. Engl.*, 1997, **36**, 2485.
7 L. Servillo, C. Balestrieri, L. Quagliuolo, L. Iorio and A. Giovane, *Eur. J. Biochem.*, 1993, **213**, 583.
8 B. Nawrot and M. Sprinzl, *Nucleosides Nucleotides*, 1998, **17**, 815.
9 (*a*) J. Plavec, W. Tong and J. Chattopadhyaya, *J. Am. Chem. Soc.*, 1993, **115**, 9734; (*b*) J. Plavec, N. Garg and J. Chattopadhyaya, *J. Chem. Soc., Chem. Commun.*, 1993, 1011; (*c*) J. Plavec, L. H. Koole and J. Chattopadhyaya, *J. Biochem. Biophys. Methods*, 1992, **25**, 253; (*d*) L. H. Koole, H. M. Buck, A. Nyilas and J. Chattopadhyaya, *Can. J. Chem.*, 1987, **65**, 2089; (*e*) L. H. Koole, H. M. Buck, H. Bazin and J. Chattopadhyaya, *Tetrahedron*, 1987, **43**, 2289; (*f*) L. H. Koole, J. Plavec, H. Liu, B. R. Vincent, M. R. Dyson, P. L. Coe, R. T. Walker, G. W. Hardy, S. G. Rahim and J. Chattopadhyaya, *J. Am. Chem. Soc.*, 1992, **114**, 9934; (*g*) J. Plavec, C. Thibaudeau, G. Viswanadham, C. Sund and J. Chattopadhyaya, *J. Chem. Soc., Chem. Commun.*, 1994, 781; (*h*) C. Thibaudeau, J. Plavec, K. A. Watanabe and J. Chattopadhyaya, *J. Chem. Soc., Chem. Commun.*, 1994, 537; (*i*) C. Thibaudeau, J. Plavec, N. Garg, A. Papchikhin and J. Chattopadhyaya, *J. Am. Chem. Soc.*, 1994, **116**, 4038; (*j*) J. Plavec, C. Thibaudeau and J. Chattopadhyaya, *J. Am. Chem. Soc.*, 1994, **116**, 6558; (*k*) C. Thibaudeau, J. Plavec and J. Chattopadhyaya, *J. Am. Chem. Soc.*, 1994, **116**, 8033; (*m*) J. Plavec, PhD Thesis, Department of Bioorganic Chemistry, Uppsala University, Sweden, 1995; (*n*) J. Plavec, C. Thibaudeau and J. Chattopadhyaya, *Tetrahedron*, 1995, **51**, 11775; (*p*) C. Thibaudeau, J. Plavec and J. Chattopadhyaya, *J. Org. Chem.*, 1996, **61**, 266; (*q*) J. Chattopadhyaya, *Nucleic Acids Symp. Ser.*, 1996, **35**, 111; (*r*) J. Plavec, C. Thibaudeau and J. Chattopadhyaya, *Pure Appl. Chem.*, 1996, **68**, 2137; (*s*) I. Luyten, C. Thibaudeau and J. Chattopadhyaya, *Tetrahedron*, 1997, **53**, 6433; (*t*) C. Thibaudeau, A. Földesi and J. Chattopadhyaya, *Tetrahedron*, 1997, **53**, 14043; (*u*) C. Thibaudeau, A. Földesi and J. Chattopadhyaya, *Tetrahedron*, 1998, **54**, 1857; (*v*) I. Luyten, C. Thibaudeau and J. Chattopadhyaya, *J. Org. Chem.*, 1997, **62**, 8800; (*w*) C. Thibaudeau and J. Chattopadhyaya, *Nucleosides Nucleotides*, 1998, **17** 1589; (*x*) I. Luyten, J. Matulic-Adamic, L. Beigelman and J. Chattopadhyaya, *Nucleosides Nucleotides*, 1998, **17**, 1605; (*y*) C. Thibaudeau and J. Chattopadhyaya, *Nucleosides Nucleotides*, 1997, **16**, 523; (*z1*) C. Thibaudeau, J. Plavec and J. Chattopadhyaya, *J. Org. Chem.*, 1998, **63**, 4967; (*z2*) C. Thibaudeau, A. Kumar, S. Bekiroglu, A. Matsuda, V. E. Marquez and J. Chattopadhyaya, *J. Org. Chem.*, 1998, **63**, 5447.
10 (*a*) H. P. M. de Leeuw, C. A. G. Haasnoot and C. Altona, *Isr. J. Chem.*, 1980, **20**, 108; (*b*) C. Altona and M. Sundaralingam, *J. Am. Chem. Soc.*, 1972, **94**, 8205; (*c*) C. Altona and M. Sundaralingham, *J. Am. Chem. Soc.*, 1973, **95**, 2333.
11 (*a*) J. Feigon, A. H. J. Wang, G. A. van der Marel, J. H. van Boom and A. Rich, *Nucleic Acids Res.*, 1984, **12**, 1243; (*b*) S. Tran-Dinh, J. Taboury, J.-M. Neumann, T. Huynh-Dinh, B. Genissel, B. Langlois d'Estaintot and J. Igolen, *Biochemistry*, 1984, **23**, 1362; (*c*) P. W. Davis, K. Hall, P. Cruz, I. Tinoco and T. Neilson, *Nucleic Acids Res.*, 1986, **14**, 1279; (*d*) P. W. Davis, R. W. Adamiak and I. Tinoco, *Biopolymers*, 1990, **29**, 109; (*e*) P. Agback, A. Sandstrom, S.-I. Yamakage, C. Sund, C. Glemarec and J. Chattopadhyaya, *J. Biochem. Biophys. Methods*, 1993, **27**, 229; (*f*) P. Agback, C. Glemarec, L. Yin, A. Sandstrom, J. Plavec, C. Sund, S.-I. Yamakage, G. Wiswanadham, B. Rousse, N. Puri and J. Chattopadhyaya, *Tetrahedron Lett.*, 1993, **34**, 3929.
12 (*a*) N. S. Zefirov, *Zh. Org. Khim.*, 1970, **6**, 1761; (*b*) N. S. Zefirov, L. G. Gurvich, A. S. Shashkov, M. Z. Krimer and E. A. Vorob'eva, *Tetrahedron*, 1976, **32**, 1211; (*c*) R. Hoffmann, *Acc. Chem. Res.*, 1971, **4**, 1; (*c*) N. D. Epiotis, S. Sarkanen, D. Bjorkquist, L. Bjorkquist and R. Yates, *J. Am. Chem. Soc.*, 1974, **96**, 4075; (*d*) K. B. Wiberg, *Acc. Chem. Res.*, 1996, **29**, 229; (*e*) W. K. Olson and J. L. Sussman, *J. Am. Chem. Soc.*, 1982, **104**, 270; (*f*) W. K. Olson, *J. Am. Chem. Soc.*, 1982, **104**, 278.
13 (*a*) F. A. A. M. De Leeuw and C. Altona, *J. Comput. Chem.*, 1983, **4**, 428 and PSEUROT, QCPE program No 463; (*b*) C. A. G. Haasnoot, F. A. A. M. de Leeuw and C. Altona, *Tetrahedron*, 1980, **36**, 2783.
14 J. E. Kilpatrick, K. S. Pitzer and R. Spitzer, *J. Am. Chem. Soc.*, 1947, **69**, 2483.
15 (*a*) E. Diez, J. S. Fabian, J. Guilleme, C. Altona and L. A. Donders, *Mol. Phys.*, 1989, **68**, 49; (*b*) L. A. Donders, F. A. A. M. de Leeuw and C. Altona, *Magn. Reson. Chem.*, 1989, **27**, 556; (*c*) C. Altona, J. H. Ippel, A. J. A. W. Hoekzema, C. Erkelens, G. Groesbeek and L. A. Donders, *Magn. Reson. Chem.*, 1989, **27**, 564; (*d*) J. van Wijk, unpublished results.

Paper 8/09350D